MOLECULAR DDYNAMICS SIMULATIONS OF DAMAGE AND PLASTICITY - THE ROLE OF AB INITIO CALCULATIONS IN THE DEVELOPMENT OF INTERATOMIC POTENTIALS.

Charlotte Becquart, Christophe Domain

MOLECULAR DDYNAMICS SIMULATIONS OF DAMAGE AND PLASTICITY - THE ROLE OF AB INITIO CALCULATIONS IN THE DEVELOPMENT OF INTERATOMIC POTENTIALS.

Journal:	*Philosophical Magazine & Philosophical Magazine Letters*
Manuscript ID:	TPHM-09-Jun-0235.R1
Journal Selection:	Philosophical Magazine
Date Submitted by the Author:	30-Jul-2009
Complete List of Authors:	Becquart, Charlotte; Laboratoire de Métallurgie Physique et Génie des Matériaux, USTL, ENSCL Domain, Christophe; EDF, MMC
Keywords:	ab initio, atomistic simulation, interatomic potential, plasticity of metals, radiation damage
Keywords (user supplied):	ab initio, atomistic simulation, interatomic potential

MOLECULAR DYNAMICS SIMULATIONS OF DAMAGE AND PLASTICITY - THE ROLE OF AB INITIO CALCULATIONS IN THE DEVELOPMENT OF INTERATOMIC POTENTIALS.

C.S. Becquart[1], C. Domain[2]

[1]Laboratoire de Métallurgie Physique et Génie des Matériaux (LMPGM), Ecole Nationale Supérieure de Chimie de Lille, UMR 8517, Bat. C6, F-59655 Villeneuve d'Ascq Cedex, France

[2]Electricité De France, Recherche et Développement, Matériaux et Mécanique des Composants, Les Renardières, F-77250 Moret sur Loing, France

1

Abstract

Predicting the behaviour of a component under irradiation or submitted to an external load often requires the understanding of the evolution of its microstructure. This usually calls for the knowledge of the mechanisms taking place at the atomic level, which are introduced in multi-scale type modelling suites. In this context, interatomic potentials are necessary ingredients in the use of most simulations techniques at the atomic level. They have been used for more than forty years in various areas of materials science and in particular in the fields of radiation damage and plasticity. These simulations have in particular shed light on the role of solute atoms in the formation of the primary damage or the motion of dislocations. However, *ab initio* calculations, as well as comparison of the results obtained with different interatomic potentials have pointed out some failures in these potentials which led to the building of new ones. This article underscores thus how *ab initio* calculations, which nowadays constitute the state of the art methods to predict atomic properties, can (and will) contribute more and more in the assessment, validation and building of interatomic potentials.

1 Introduction

Simulations of metals and metallic alloys using atomic level techniques such as Molecular Dynamics (MD) are necessary in many areas of materials science. Indeed, the macroscopic properties of matter are intimately linked to the local atomic configurations of the atoms and the way they evolve with time or under some external constrains. As a result, mesoscopic and macroscopic models used to investigate the behaviour of a component in a particular environment (temperature, pressure, mechanical loading, irradiation ...) or the evolution of a microstructure rely more and more on data or laws which have been obtained at the atomic

[1] Contact author : charlotte.becquart@univ-lille1.fr

scale. However to simulate a piece of materials of relevant size, one has to use what is called empirical interatomic potentials which are nothing more than mathematic functions which describe the forces felt by the atoms, forces due to neighbouring atoms and their electrons. The validity of the results obtained in such simulations depends thus on the potential used and the relevance of the potential to investigate a given situation has to be properly established. The first simulations relied on pair potentials,[2] which presented a certain number of limitations. For example, pair potentials fail to accurately describe situations in which the electronic density varies (close to surfaces, extended defects...), and are furthermore not really appropriate to model metallic bonding. In the 80's a big step forward was achieved with the birth of many body potentials such as the Embedded Atom Method (EAM) [1], Finnis Sinclair [2], effective medium [3] and other similar types [4] [5] [6] potentials. Since then, numerous problems have been investigated with the help of MD, so numerous in fact that searching for the key words "molecular dynamics" in a ISI web of Knowledge type of data-base search engine returns more than 100 000 answers. This literature review provides a picture of the required features in developing interatomic potentials. We focus on the simulation of conditions relevant to radiation damage and material plasticity. In the first part, results obtained in these fields for Fe alloys are presented. In the second part, we underscore some key issues of the interatomic potentials revealed by the comparative use of different potentials for a given problem or by the spreading use of *ab initio* calculations. The third part underscores the increasingly significant role of *ab initio* calculations in the assessment, validation and building of interatomic potentials. A final paragraph brings to the fore some issues related to the comparison between simulations and experimentally obtained data.

Deleted: mimic
Deleted: the other
Deleted: s
Deleted: drawbacks, for instance in cases where
Deleted: or
Deleted: In this paper,
Deleted: w
Deleted: the use of empirical potentials in
Deleted: oriented problems
Deleted: a
Deleted: a

2 The use of interatomic potentials to investigate radiation damage and plasticity

2.1 Displacement cascades in Fe alloys

MD has been used for almost fifty years to simulate the displacement cascades initiated by the neutrons when they interact with matter since the pioneering work of Gibson and co-workers [7]. Fe, because of its industrial role, is one of the most investigated materials and displacement cascades have been modelled in pure Fe for more than 45 years [8] [9] [10] [11] [12] [13]. The aim of all these simulations is to obtain the defect population distribution obtained by a Primary Knock on Atom (PKA) of given energy. The simulations are done in

Deleted: ed

[2] the total energy of the system is obtained as a sum of interactions between pairs of atoms, the energy depends only on the distance between the two atoms of the pair considered and not on their environment.

the micro canonical ensemble with periodic boundary conditions as in for instance [14], or at constant pressure [9] [11].

The damage production has been simulated for specific Fe alloys chosen both because of their industrial interest but mainly because interatomic potentials for these alloys were available. Because of the predominant role of Cu in the embrittlement of the pressure vessel steels discovered more than forty years ago [15], the first simulations of displacement cascades in dilute Fe alloys were done in Fe-Cu dilute alloys [16] [17] [18]. Despite its notorious role in steels, the influence of C in solution was studied only recently by Calder *et al.* [19] [18] certainly because of the lack of reliable Fe-C potentials. Another interstitial species of great interest, specially in the case of materials for fusion application, is He, and its influence on the primary damage in Fe is now the subject of extensive work [20] [21] [22] [23] [24] [25]. Phosphorous is well known for its embrittlement properties and Fe-P alloys were modelled by Hurchand *et al.* [26]. Finally high-Cr ferritic/martensitic steels are candidate structural materials for key components in most future nuclear options due to their superior mechanical properties and good radiation resistance. Fe-Cr alloys being representative of such steels are now being extensively investigated, see for instance [27] [28] [29] [30] [31] [18]. Let's now summarise the main results obtained about the influence of solute atoms on the primary damage in Fe as predicted by these simulations.

Case of Fe–Cu

MD simulations of displacement cascades in pure Fe, Fe-0.2at.%Cu and Fe-2at.%Cu were done with different PKA energies [16]. The typical defects (vacancies and interstitials) appeared during the cascade process and most of them recombine in the first few picoseconds. In the time scale covered by the MD simulations, the presence of Cu atoms did not seem to influence in an obvious manner the primary damage as compared to the damage obtained in pure Fe. The number of residual defects was similar and fell within the range of the data, with a similar tendency to form point defect clusters. However, a tendency to form mixed objects (vacancies or interstitials gathered with Cu atoms) was noticed in the Fe-2at.%Cu. Calder *et al.* [17] who studied 1at.%Cu observed also a slight tendency to form Cu–V pairs. In neither case were Cu precipitates, or dilute atmospheres observed to form.

Case of Fe–C

Displacement cascades were simulated at either 100 or 600 K, with energy in the range 5-20 keV, in iron containing carbon in solution, with concentrations in the range 0-1 at.% [19]. It was found that C in solution had no discernible effect on the primary damage, i.e. on the number of defects produced in cascades or on the clustered fraction of either self-interstitial

Deleted: 9
Deleted: 9
Deleted: 11
Deleted: 11
Deleted: put forward
Deleted: 18
Deleted: 18
Deleted: numerous
Deleted: 18
Deleted: 18
Deleted: 16
Deleted: 16
Deleted: . Most of the defects
Deleted:
Deleted: amount
Deleted: lied in the scattering
Deleted: the
Deleted: also
Deleted: 17
Deleted: 17
Deleted: noticed
Deleted:
Deleted: s
Deleted: 19
Deleted: 19
Deleted: as well as

atoms (SIAs) or vacancies. It was however observed that significant fractions of single SIAs and vacancies were trapped by C atoms in the cascade process, irrespectively of cascade energy. The fraction of vacancies trapped was independent of temperature, but because of their high mobility, the fraction of SIAs trapped increased strongly with temperature.

Case of Fe–He

Displacement cascades were simulated in α-Fe containing different concentrations of substitutional He atoms [18] [22]. The simulations were done at 100K with PKA energies ranging from 0.5 to 5 keV. The concentration of He in Fe varied from 1 to 5 at%. It was found that the total number of point defects produced increased with increasing He concentration. He-vacancy clusters were observed to form in the cascades, and the production efficiency of He-vacancy clusters increased with increasing He concentration and PKA energy. However, the mean size of He-V clusters was found to be independent of temperature for the same He concentration and recoil energy.

An influence of He on the production of defects and their subsequent clustering was also reported in [23] and [24]. Furthermore these simulations revealed that the location of the He atoms, in substitutional or interstitial positions, played a major role. Compared to pure Fe, interstitial He atoms appeared to increase the amount of Frenkel pairs generated during the cascades, while substitutional He atoms tended to decrease this production. However, in both cases, He atoms stabilized larger SIA clusters, due to a strong binding energy. Because of this strong binding energy, He atoms can trap SIA clusters and thus slow down their subsequent migration. The number and size of the SIA clusters was found to increase with the PKA energy and temperature.

Case of Fe–Cr

Displacement cascades up to 50 keV in Fe and Fe–Cr (with the range of Cr concentration varying between 5, 10 and 15 at. %) were simulated by a number of groups [27] [28] [29] [30] [31]. These simulations all showed that the main effect of the presence of Cr in the system was the preferential formation of mixed Fe-Cr dumbbells and mixed interstitial clusters, with expected lower mobility than in pure Fe, in agreement with some experimental indications. The presence of Cr did not significantly influence either the ballistic phase of the cascade, or the primary damage state, in terms of number of surviving defects or clustered fraction. The influence of the potential on the vacancy clustered fraction and quantity of mixed Fe-Cr dumbbells was once more emphasized in [29] and [30].

The trends observed in Fe–Cu, Fe–C and Fe–Cr alloys were confirmed in a recent work using Modified Embedded Atom Method (MEAM) potentials [18] to study the effects of alloying

Deleted: of the SIAs
Deleted: 18
Deleted: 18
Deleted: 22
Deleted: 22
Deleted: s
Deleted: on
Deleted: s
Deleted: The
Deleted: noticed
Deleted: by
Deleted: 23
Deleted: 23
Deleted: 24
Deleted: 24
Deleted: it was
Deleted:
Deleted: self-interstitial
Deleted: Some He-vacancy clusters were generated in the core of the displacement cascades but also at the periphery of SIA clusters
Deleted: .
Deleted: interstitial
Deleted: d
Deleted: 27
Deleted: 27
Deleted: 28
Deleted: 28
Deleted: 29
Deleted: 29
Deleted: 30
Deleted: 30
Deleted: 31
Deleted: 31
Deleted: , with expected lower mobility than in pure Fe
Deleted: .
Deleted: 29
Deleted: 29
Deleted: 30
Deleted: 30
Deleted: 18
Deleted: 18

elements, on the number of residual point defects (vacancies and interstitials), their clustering tendency and configuration.

Case of Fe–P

Displacement cascades with PKA ranging from 1 to 16 keV in a Fe–0.04at.%P matrix and in pure Fe were compared to investigate the interaction of the phosphorus atoms with the radiation [26]. The results were similar to those obtained in the Fe–Cr alloys. It was observed that the P atom in the Fe matrix did not increase significantly the damage induced and that the density of vacancies and the morphology of the clusters formed in the Fe–0.04at.%P system were indistinguishable from residual defects produced in a pure irradiated Fe matrix. The influence of P was mainly on the SIAs, as the displacement cascades induced the formation of mixed dumbbells or Fe–P nano-clusters. Nearly 35% of the atoms which were ejected from the core region of the cascade during the ballistic phase formed such solute-defect clusters which remain pinned over the period of several hundred picoseconds.

The overall picture which emerges from this brief overview is that the solute atoms investigated so far do not seem to have much influence on the primary damage in terms of defect density or clustered fractions. A possible explanation for this fact, is that all the elements considered in these simulations are light elements or elements with masses close to that of Fe (Mass He = 2 a.m.u., C = 12 a.m.u, P = 30 a.m.u, Cr = 52.00 a.m.u, Cu = 63.55 a.m.u). Furthermore, the elements whose mass are the most different from that of Fe are present in very small quantities. The most concentrated solute are Cr atoms whose mass is very close to that of Fe (Fe = 55.85 a.m.u.). The presence of the solutes in the Fe matrix will not thus influence the ballistic phase of the displacements cascades as opposed to what could be expected from elements with larger masses as was pointed out by Calder *et al.* [32] who investigated the effect of the PKA mass on the damage produced in individual cascades. Furthermore, MD can only simulate the ballistic processes taking place when a recoil atom is ejected from its lattice position and no real diffusion can take place in the timescale covered by MD.

However, if one is interested in simulating the longer term evolution of the primary damage using for instance Kinetic Monte Carlo algorithms, the solute atoms, if they bind strongly to the point defects, have to be explicitly accounted for in the simulations. Indeed it is fairly obvious that bound defects (V–He, V–C or mixed dumbbells) will not migrate at the same speed as pure vacancies or SIAs. This is specially the case for solute atoms such as P and Cr which bind very strongly with SIAs as evidenced by *ab initio* calculations [33][34].

Deleted: 26

Deleted: 26

Deleted: is

Deleted: little amount

Deleted:

2.2 plasticity of Fe alloys

MD was also used in the 70's to study dislocation properties at the atomic scale in a wide range of metals because the nucleation of dislocations and their motion play a key role in metal plasticity. Static calculations were performed to investigate the core structure which controls many properties of the dislocations. Indeed, for edge dislocations in Zr, the core properties and the critical stress for dislocation glide (Peierls stress) were found to depend sensitively on whether the core extends or not **[35],** while for screw dislocations, the issue of whether the core is degenerate, i.e. asymmetrically spread in the three {1 1 0} planes of the [111] zone or compact will drastically change the dislocation properties. The core of a dislocation structure can be characterized using the differential displacement method proposed by Vitek **[36]** **Figure 1** represents the two very much debated structures of the screw dislocation core. Note that in the case of body centred cubic (bcc) metals, most interatomic potentials predict that the screw dislocation core is degenerate as in Fig.1a; this issue will be discussed further in the paper.

Insert **Figure 1** around here

With the increase of computing power, the mobility of dislocations under stress or strain as well as their interactions with some defects and in particular irradiation related defects have been investigated in the past ten years **[37] [38] [39] [40] [41]** leading to many important results and data useful for multi-scale modelling purposes. As the aim of the present paper is not to review them, rather, the following paragraphs summarise a few of the significant achievements obtained recently in the case of pure Fe or dilute Fe alloys in this field.

Dislocation – carbon interaction in Fe

Many properties of steels depend on their carbon content which has been shown to segregate at the core of dislocations forming what are called Cottrell atmospheres. The formation of such atmospheres may be a serious drawback, since they will modify the stress which needs to be applied to make the dislocations move.

An FeC potential was developed in **[42]** based on *ab initio* data related to the interactions of carbon with point defects as well as with other carbon atoms **[43]**. As a result, the deformation of the octahedral site as well as the C migration energy (via the tetrahedral site) found by *ab initio* were correctly reproduced by this potential. Using the energy barrier variation as a function of the applied stress, this newly developed potential was used to model the Snoek peak observed in internal friction experiments **[44]**. For this matter, saddle point energies for

Deleted: has
Deleted: been
Deleted: as
Deleted: s
Deleted: the
Deleted: d
Deleted: structure
Deleted: representation for atomic differential displacements as illustrated in
Formatted
Deleted: d
Deleted:
Formatted
Deleted: then
Deleted: T
Deleted: will thus only
Deleted: but
Deleted: s
Deleted: have
Deleted: is

the diffusion of carbon, evaluated under uniaxial stress by molecular statics, were introduced in a kinetic Monte-Carlo scheme to predict the repartition of carbon atoms in the different octahedral sites. This approach led to quantitative predictions of the internal friction, in good agreement with the experiment results.

Furthermore, the potential was used to model the interaction of C atoms with a screw and an edge dislocation and compare them with the predictions of anisotropic elasticity theory [45]. It was shown that if the interaction of C with dislocation far from the core is purely elastic, close to the core the local change of the bcc crystal structure is more complex and does not follow the results of elasticity theory. Moreover, a quantitative agreement was obtained between both modelling techniques when anisotropic elasticity calculations were performed and both the dilatation and the tetragonal distortion induced by the C interstitial were considered. Finally, the binding energy between a single C atom and a dislocation was found to be E_{bind} = 0.66 eV for an edge dislocation and E_{bind} = 0.41 eV for a screw dislocation, in reasonable agreement with the available experimental results.

Screw dislocation mobility in Fe

In materials with relatively high lattice friction (e.g. bcc and hcp metals) the flow stress is strongly temperature dependent and at low temperatures, the deformation is mainly controlled by the motion of screw dislocations which move slower than edge dislocations (see for instance [46] for a review on the subject). The mobility of screw dislocations which occurs through the nucleation and the propagation of double kinks (DK) [47] is therefore expected to control the plastic flow in iron. The strong temperature dependency of the flow stress in iron arises from the fact that the DK mechanism is a thermally activated process which was investigated in detail in [39]. In this latter work, MD simulations were used to study the mobility of a a/2⟨111⟩ screw dislocation in iron submitted to a pure shear load at different temperatures and to determine the critical resolved shear stress. For this purpose, the potentials developed recently for pure Fe by Mendelev *et al.* and Ackland *et al.* [48, 49] were used as they reproduce correctly the compact core structure of the screw dislocation in Fe in agreement with *ab initio* results. It was found, that under a constant rate shear strain applied on (110) planes, the glide of the screw dislocations does take place on (110) planes and is occurring through the nucleation and the propagation of DK along the dislocation line as illustrated on **Figure 2**.

Insert **Figure 2** around here

Deleted: The occurrence of C atoms induced an anelastic deformation in the lattice which was then determined by MD.

Deleted: obey a priori to the

Deleted: Furthermore

Formatted

Formatted

Deleted: *D*

Deleted: s

Deleted: 39

Deleted: 39

Deleted: as

Deleted: it

Deleted: s

Formatted

The critical stresses required to move the dislocation were to be substantially larger than the critical stresses found in experiment. However, it was shown that the discrepancy between experimental and simulated critical stresses was due to the fact that the parameters involved in the thermal activation process, i.e. the dislocation length and the applied velocity are totally different in the experiments as compared to the simulations. Accounting for these different conditions lead to critical stresses in very good agreement with experiments. These simulations underscore nicely the power of MD to give a detailed and quantitative characterisation of the motion of the screw dislocation if the interatomic potential is appropriate. Indeed, simulations performed with potentials predicting the wrong core structure (i.e. the degenerate core) led to the prediction of critical stresses that were too high **[50].**

Screw dislocation – irradiation defect interactions in Fe

The accumulation of point defects and small point defect clusters formed in the displacement cascades leads to the formation of vacancy clusters, i.e. nano-voids as well as interstitial clusters: dislocation loops with Burgers vectors along ⟨100⟩ and ⟨111⟩ directions in Fe. These features lead to some hardening of the materials due to their interaction with dislocations.

These interactions have been characterised by MD by numerous groups and a thorough review can be found in [**51**] and references therein. This review covers the interactions of edge and screw dislocations in fcc metals as well as those of edge dislocations in Fe. Static calculations of the interaction of the ⟨111⟩ screw dislocation with a large number of irradiation induced defects in Fe can be found in [**52**]. To complement the results exposed in [**51**] and [**52**], we present here the results of some recent dynamics calculations we have performed regarding the interaction of the ⟨111⟩ screw dislocation in Fe with nano-voids and dislocation loops and obtained with the Fe potential developed by Mendelev *et al.* [**48**]. The dislocation motion was obtained using the method exposed in the section dedicated to the study of the screw dislocation glide. At the beginning of the simulation, the defect (i.e. the nano-void or the dislocation loop) is positioned in front of the dislocation. A pure shear is applied to the simulation box which makes the dislocation move. When the dislocation reaches the defect, it becomes pinned and bows out, until a critical stress and a critical angle are reached. **Figure 3** illustrates the dislocation line configuration just before the dislocation unpins for a nano-void containing 200 vacancies **(Fig.3a)** and for a ⟨111⟩ interstitial loop containing 61 SIAs **(Fig.3b)** at 300K.

Insert **Figure 3** around here

Deleted: found, in a first approach,
Deleted:
Deleted: Taking into a
Deleted: allowed to obtain
Deleted: d
Formatted
Formatted
Formatted
Deleted: 51
Deleted: 52
Deleted: 48
Formatted

The curvature difference between the two cases is significant and indicates that the dislocation loop is a stronger defect than the void, as the critical angle is smaller for the loop. Another interesting feature, is that the screw dislocation interaction with the SIA loop induces the formation of an helicoidal turn during the absorption of the loop by the dislocation as was proposed by Hirsch [53]. The unpinning of the screw dislocation is then due to the release of the dislocation loop. Similar simulations at different temperatures indicate that as could be expected, thermal energy decreases the critical stress needed to unpin the dislocation.

Formatted

Formatted

3 Short comings of the interatomic potentials: what may be missing

We now discuss some of the short comings of the interatomic potentials brought to the fore either by the use of different interatomic potentials in a given situation or by the comparison of the simulation results with experimental data.

3-1 case of radiation damage

Because of the short and small spatial dimensions of displacement cascades, very few experimental results are available on primary damage. The exception is the case of W which was investigated with the help of a field ion microscope **[54][55].** However, in the case of Fe and Fe alloys, no such data are available and it is a non trivial task to try to assess the validity of the results obtained. A careful study using three different interatomic potentials found in the literature indicated that the primary damage, i.e. the amount and structure of the defects produced can be very sensitive to the potential **[14]** as illustrated on **Figure 4**.

Deleted: time length space

Deleted: the

Deleted: the

Deleted: is very much

Deleted: sensitive

Deleted: 14

Deleted: 14

Deleted: 3

Formatted

Insert **Figure 4** around here

Some characteristics of the potentials, not always taken into account in the fitting procedure of the potentials, were correlated to the type of damage produced by displacement cascades. Equilibrium properties (for instance the atom Mean Square Displacements, the vacancy migration and vacancy-vacancy binding energies) appeared to have some influence on the damage production. Moreover, it was also found that the repulsive part of the potential has a non negligible influence on the cascade morphology. This issue is more problematic as demonstrated in what follows. Interatomic potentials are usually adjusted based on equilibrium properties, and are expected thus to model correctly the behaviour of the forces acting on the atoms when they are separated by distances close to or above the first nearest neighbour distance. To make these potentials suitable for displacement cascade simulations, it is necessary to modify the short-range part corresponding to close encounters, which take

Deleted: to

place during the ballistic phase of the cascade. In the process, screened Coulomb potentials such as the Ziegler-Biersack-Littmark ZBL potential [56] are usually used at very short ranges (r less than 1 Å) while for intermediate ranges, one typically utilizes Born-Mayer-type potentials similar to that published by Maury *et al.* [57]. The different functions are joined by smooth interpolation schemes and continuity between different branches is ensured at the knot points up to their first derivatives. This "hardening" of the potentials is usually validated by making sure that they reproduce the threshold displacement energies of the materials[3]. These threshold displacement energies are usually the only parameters fitted to during the hardening process, they are therefore the only physical quantities giving insight on the very short distance interactions which are taken into account in the fitting procedure. However it was shown that predicting threshold displacement energies in agreement with the experimental data is not sufficient to characterize very short distance interactions as the three potentials examined in [14] predicted very similar displacement threshold energies while producing significantly different primary damage as can be seen in **Fig. 4.** Moreover, using screened Coulomb potentials, Becquart *et al.* [58] [59] showed that the shorter the range, the lower the focusing threshold and the more important the Replacement Cascade Sequences (RCS) production. The cascade expansion and density was found to be quite sensitive to the potential range at high interaction energies, and the overall cascade expansion found to be governed by the 10% highest-energy recoils which energy is above the RCS focusing energy threshold. The cascade density, i.e., the number of transient defects produced per unit volume, was found to be sufficient to interfere significantly with RCS propagation and thus with the spatial distribution of Frenkel pairs. It was concluded that a careful choice of the short-range potential has thus to be made when simulating displacement cascades. Later on, a number of displacement cascades of energy ranging from 5 to 40 keV were simulated using the same procedure with four different interatomic potentials for α-Fe, each of them providing, among other things, varying descriptions of self-interstitial atoms (SIA) in this metal [60]. The behaviour of the cascades at their different phases and the final surviving defect population was studied and compared. In this study, the influence of the short-range part of the potential was also found to be non negligible as well as the mobility of the point defects. The stability of the SIAs and their migration properties involve atomic distances closer to the first nearest neighbour distance. For instance, in a Fe dumbbell, the two atoms are separated by 1.91 Å (VASP results for a 54 atom supercell) which corresponds to 0.771 nearest-neighbour unit

Deleted: of potential "hardening"

Deleted: dure

Deleted: was

Deleted: 14

Deleted: 14

Formatted

Deleted: 3

Formatted

[3] The threshold displacement energy is the minimum kinetic energy one must give an atom to create a stable

[61]. When the SIA migrates, the distance between the atoms can be as small as 2 Å, while during the ballistic phase of a collision cascade atoms may get as close as close to 1 Å. It is thus necessary to reproduce correctly the forces felt by the atoms when they are in these interatomic distance ranges. The role of SIA properties on the prediction of the damage was revisited by Bjorkas and Nordlund [62] who used three potentials developed for Fe, all of them describing the interstitial energetics correctly. The results showed that the total Frenkel pair production was the same within the statistical uncertainty for the three potentials, but also that some differences remained in the fraction of clustered defects. However, these differences were smaller than those predicted by previous potentials. In this last study, note that two of the three potentials were "hardened" following the same procedure, which corroborates the conclusions made previously on the role of the high energy recoil range of the potential.

For potentials intended to be used to investigate radiation damage, it appears thus that some care should be taken regarding the properties of SIAs as well as the fitting of the potential in the range of atomic spacings corresponding to high energy recoils and it will be shown further in the text how *ab initio* calculations can help in that matter.

3.2 case of dislocation properties

For potentials dedicated to the study of plasticity, two other properties appear to have some relevance: the stacking fault energy and the core structure of the dislocations. The elastic properties such as the elastic constants, which are important properties of the materials, are usually well reproduced by the interatomic potentials and are in fact very often used as fitting input parameters. The stacking fault energy, in the other hand, which is related (even if in a non trivial way) to the dislocation glide properties, is often incorrectly predicted by the interatomic potentials. One typical example is the family of the hexagonal close packed (hcp) metals from the IIB column in the periodic table such as Zr or Ti. These metals are anisotropic and the glide properties of dislocations in basal or prismatic planes are different. Experimental observations indicate that for these elements, slip is more favourable in the prismatic plane than in the basal one, however most empirical potentials usually predict a lower stacking fault energy for the basal plane. In such a case, *ab initio* calculations can provide much needed insight, as will be demonstrated in the next section.

Another key property of the dislocations which plays a role on their mobility is their core structure. Experimentally the observation of the core structure even with high resolution

Deleted: which
Deleted: ed
Deleted:
Deleted: the
Formatted
Deleted: ompliances
Deleted: that
Deleted: that
Deleted: light can be shed using
Deleted: paragraph

Frenkel pair in the lattice. It depends on the materials and on the orientation of the primary recoil.

microscopy is difficult except for materials where the dislocation core is dissociated, i.e. low stacking fault energy materials. In that case also, *ab initio* calculations are very relevant, as they indicate, for instance, that in the case of body centred cubic materials, like Fe, the core of the screw dislocation is compact [63] [64] rather than degenerate as predicted by most Fe potentials.

4. The use of *ab initio* calculations in the assessment of empirical interatomic potentials and for the development of new potentials

One of the big steps forward in the field of interatomic potentials is the use of *ab initio* data to assess the validity of existing potentials and, if necessary, build new ones. In what follows we present a short review of some of the key properties which have been revisited recently thanks to *ab initio* results.

In the field of radiation damage, interatomic potentials used for years to simulate α-Fe were called into question when *ab initio* calculations [61] showed that the rotation energy from the ⟨110⟩ to the ⟨111⟩ SIA configuration might be higher than 0.7 eV (to be compared to the "close to 0.1 eV" predicted by empirical many-body potentials used at that time [65], [66]). Indeed, according to MD simulations with empirical interatomic potentials, two regimes of single SIA migration had been broadly identified (see e.g. [67]). At low temperatures, it was found that the SIA spent a significant time in a ⟨110⟩ dumbbell configuration, followed by a series of fast jumps in one direction, via the ⟨111⟩ crowdion mechanism, while at high temperatures, the SIA migration approached a full 3D regime. The simulations provided an effective migration energy of the single SIA between 0.04 and 0.08 eV, depending on the interatomic potential used [67]. The energy needed for change of ⟨111⟩ direction was found to be between 0.1 and 0.3 eV [68], [69] [70] [65].

This picture stood in contrast to the experimental data which suggested that the migration (and rotation) energy of the SIA is close to 0.3 eV ([71] [72] and references therein). Furthermore, the *ab initio* calculations of [61] indicated that the rotation from the ⟨110⟩ configuration to the ⟨111⟩ configuration which, according to the MD simulations presented above, governs the migration mechanism of SIA in Fe, was highly unlikely as too costly. Moreover, another migration mechanism, proposed already 40 years ago by Johnson [73], involving both a rotation (a change of ⟨110⟩ direction) and a migration (a jump to first nearest neighbour) was three years later found to be more plausible [74]. These later *ab initio* results obtained by another group and with another *ab initio* model confirmed that the energy

Deleted: d
Deleted: the
Deleted: the
Deleted: the
Deleted: ing of
Deleted: new
Deleted:
Deleted: 61
Deleted: 58
Deleted: 67
Deleted: 64
Deleted: 65
Deleted: 62
Deleted: did
Deleted: with
Deleted: 61
Deleted: 58

difference between ⟨110⟩ and ⟨111⟩ SIA configuration is of the order of 0.7 eV, and that the migration of the SIA should take place according to Johnson's model with a migration energy of 0.34 eV in agreement with the experimental results of Takaki [72].

Because of the importance of point defect properties and in particular of the SIA as presented above, specially when one wishes to model radiation damage, a new potential for α-Fe was derived in 2004 [49]. This potential was adjusted to fit *ab initio* data, and a great care was taken about the relative stability of the dumbbells [61]. It is nowadays commonly admitted to be the state of the art potential for this material [75]. Terentyev and coworkers [76], using this newly derived potential, showed that it provides a dynamic migration energy for the single SIA in agreement with the experimental value. As stated previously, the use of this potential to simulate displacement cascades did not lead to tremendous differences in the amount and type of primary damage created as compared to what had been obtained with the previously used potentials [62] [60] and in that regards, the "old" potentials are perfectly acceptable. However, if one uses the potentials to investigate the evolution of the primary damage with time, or the behaviour of dislocation loops as was done in [77], it becomes necessary to reproduce correctly the properties of the SIAs.

Note that it is now possible to use *ab initio* calculations and more specifically *ab initio* molecular dynamics simulations to determine threshold displacement energies. It has been done in covalent materials SiC [78] and Si [79] and a good agreement was obtained between the experimental data available and the calculated ones. The use of *ab initio* MD can allow to explore more precisely the direction dependence of the threshold energies. Furthermore, in the case of alloys, the determination of these energies for each species will be straightforward.

It turned out that, probably because of the care taken to fit properly the short range interaction distance which is representative of the state felt by the atoms in the neighbourhood of interstitial atoms, the newly built potential also predicted the core structure of the 1/2a⟨111⟩ screw dislocation to be compact (Fig.1b) in agreement with *ab initio* results and in contrast with the older potentials.

There are two possible configurations for 1/2a⟨111⟩ screw dislocations in bcc materials, corresponding to the so called "easy" and "hard" configurations [80]. The "easy" configuration was found to be more stable with the newly built potential than the "hard" one [39] and all "hard" screw dislocations thus relaxed into an "easy" one. As mentioned previously, this potential was used to determine the critical stresses necessary to make the

Deleted: dumbbells
Deleted: 72
Deleted: 69
Deleted: 49
Deleted: 49
Deleted: on
Deleted: 61
Deleted: 58
Deleted:
Deleted: 62
Deleted: 59
Deleted: 60
Deleted: 57
Formatted
Formatted
Formatted
Deleted: a
Deleted:

1/2a⟨111⟩ screw dislocation move in α- Fe and good agreement was found with the experimental results.

Another important achievement based on the results of *ab initio* calculations is the development of potentials more appropriate to study the plasticity of hcp metals from the IIB column. In Zr, recent *ab initio* calculations **[81]** have shown that the prismatic stacking fault energy is lower than the basal one, while the potentials developed more than ten years ago, see for instance **[82][83][84]** and used up to now to study Zr all predict that the basal stacking fault energy is very low and moreover, much lower than the prismatic one. This low basal stacking fault energy can be explained by the fact that the coordination of the first nearest neighbour atoms in the basal fault is the same as that of a perfect hcp crystal. The same problem was found to apply to Ti also: the stacking fault energies of the potential developed by Girshick *et al.* **[85]** **[86]** are different than the *ab initio* data of Domain *et al.* **[87]**. Note that these results had been predicted in the past by tight binding calculations **[88]** which pointed out that the ratio of the basal to prismatic stacking fault energies is an oscillating function of the filling of the d shell. These calculations, which were in agreement with the main glide systems observed experimentally, brought to the fore the predominant role of the electronic structure of the metals in determining the main glide systems. However, to our knowledge this information was not taken into account in the building of EAM potentials until very recently. Indeed, following the *ab initio* results of **[81]**, a new Zr potential **[89]** was developed in 2007, which included these stacking fault energies as input parameters in the optimisation procedure. The newly built EAM potential predicts stacking fault energies in agreement with the *ab initio* calculations and has been used to study the plasticity of Zr **[90]**. With this new potential, prismatic slip of the screw dislocation is now observed in agreement with the experimental observations **[90]**.

Note that *ab initio* calculations, as all numerical methods, have limitations and uncertainties which must be kept in mind. Specially when the data they provide are used to assess the validity of other models such as empirical potentials for instance. It is important to keep in mind that when choosing a functional for exchange-correlation, the "A" in the acronyms GGA or LDA stands for Approximation. The choice of the functional can lead to very different results as is well known for Fe for instance. Indeed, the LDA predicts that the stable configuration for Fe at low temperature is non magnetic and has a face centred cubic structure in complete disagreement with the experimental facts. This problem can be solved by the use of GGA instead of LDA, but no clear answer as why LDA fails in this respect has been provided so far.

Deleted: a
Deleted: also initiated by
Deleted: ncy
Deleted: ies
Deleted: c
Deleted: ontrast with
Deleted: ic
Deleted: o
Deleted: F
Deleted: 81
Deleted: 74
Deleted:
Deleted: es
Deleted: now
Deleted: was
Formatted
Deleted: 90
Deleted: 87
Deleted:
Formatted

To simulate large systems, one usually considers that the core electrons are frozen. These kind of simulations are less computationally demanding than the so-called "all electron" methods such as the Linearized Augmented Plane Wave (LAPW) method. Another tricky problem is then the choice of the local basis set or in the case of plane-wave basis set, the choice of the pseudo potentials. In the case of dilute Fe alloys, it is assumed for instance that the Projector Augmented Wave (PAW) formalism should theoretically give better results than the Ultra-Soft Pseudo Potentials (USPP) formalism as it describes better the core electrons. However, the results of **Table 1** lead one to conclude that this is not always the case.

Insert **Table 1** around here

Formatted

For the Fe-Cu system, the mixing energy is higher with the PAW method than with the USPP one. Using a Metropolis algorithm, we determined the solubility limits corresponding to the mixing energies. The mixing energy of 0.82 eV leads to a solubility limit inferior to 0.001 at.% at 500 °C whereas the mixing energy of 0.55 eV leads to a solubility limit of 0.07 at.%, which is close to the experimental value of 0.1 at.% [**91**].

For the Fe-Ni system, the mixing energy obtained with the USPP method is negative (–0.12 eV) while it is positive with the PAW one (0.24 eV). In the FeNi phase diagram, the $FeNi_3$ phase exists even if it is not very stable. This means that the Fe-Ni bond is slightly more favourable than the Ni-Ni one. Consequently, the mixing energy should not be positive.

Thus for the two cases mentioned above, the USPP seems to give more reasonable results.

However for the Fe-Mn system, the binding energies between two Mn atoms both in first and in second nearest neighbour obtained with the PAW method are more in agreement with the phase diagram than those obtained with the USPP method, because of the quasi ideal character of the FeMn solution. From these examples, it appears clearly that it is difficult to assess which method gives the most precise or even correct results, except for the magnetic moments, where PAW seems to give better values than USPP since the magnetic moments are closer to those obtained with the LAPW method [**92**].

Formatted

Formatted

Another possible limitation of these calculations is the accuracy of the total energy and atomic forces prediction when atoms are very close to each other. This situation may be encountered in calculations involving SIAs, and threshold displacement energies, if ones uses pseudopotentials, as the "core" of the atoms may overlap. Here also, the use of "all electron methods" for some carefully chosen configurations can be necessary as a possible validation.

Formatted

5 Comparing the simulated results with experiments

The best way to validate the properties of an interatomic potential is to compare the results with experimental data. One problem which needs to be mentioned here is that the comparison is not always straightforward. As was said previously, in the case of displacement cascades, because of their lifetime and their spatial dimensions, no direct visualization can be done and thus no direct comparison of the simulations with experimental data is possible. Most of the time, the results obtained at the atomic level need to be introduced in higher scale codes to obtain information directly comparable with experimental data. For instance, the primary damage obtained using MD can be used in kinetic Monte Carlo models to simulate an irradiation and in this case experimentally resolvable defects and microstructures can be obtained. However, if a disagreement is found between the results of the simulations and the experimental data, it is not easy to determine the origin of the discrepancy as more than one model is involved in obtaining the final result. Similarly, agreement with data does not prove anything in this case.

Another issue is the fact that most of the models (specially in the case of simulations at the atomic level) are "infinitely" pure alloys containing no impurities of any kind, while real materials, even the purest ones, always contain impurities (not to mention point defects and larger defects such as dislocations, grain boundaries, twins and so on). One of the notorious cases is the influence of impurities such as C or N on the vacancy migration energy in pure Fe. Depending upon the author, the vacancy migration energy obtained from experiments ranged from a value of 0.55 eV [93] to 1.28 eV [94]. This discrepancy is most certainly due to the presence of very small amounts of impurity atoms (most probably C or N atoms) that, because they bind strongly with the vacancies [43], modify their mobility and thereby their diffusion coefficient. Indeed the 0.55 eV value was determined from experiments performed on a high purity α-Fe [93].

Finally, another point worth mentioning is that many "experimentally determined" properties rely on models necessary to analyse the experimental data. For instance, the migration energies of point defects can be determined from recovery experiments. In these kinds of experiments, the materials are first irradiated at very low temperatures. Most of the time, the irradiating particles are electrons, so the damage created is simple. The irradiated materials are then isochronally annealed at a specific rate and their recovery is analysed either by electrical resistivity, magnetic after-effect or internal friction measurements. In the case of pure Fe, the recovery experiments of Takaki *et al.* [72], or those of Maury *et al.* [57] are often

Deleted: ¶

Deleted: atomistic

Deleted: atomistic

Deleted: most pure

Deleted:

Deleted: s

Deleted: 93

Deleted: 84

Deleted: as

Deleted: 72

Deleted: 69

Deleted: 57

Deleted: 54

taken as a reference. The differential isochronal resistivity recovery spectra exhibit a certain number of peaks which can be associated with several processes implicating the different point defects and their clusters. Depending on which peak is associated with which point defects, different migration energies can be obtained: the same experimental data analysed by two different models can thus lead to different results.

To conclude on this subject, the best way to assess the validity of results obtained with empirical interatomic potential is to compare them with experimental results, however this is not always possible and *ab initio* calculations are a very good alternative (not to mention the fact that they are much less costly than experiments).

6. Conclusions

Simulations at the atomic level are relevant in many areas of materials science. They are nowadays commonly used in the field of radiation damage and plasticity and many interesting results have been obtained. However, the relevance of the results depends on the validity of the interatomic potentials which describe the interactions between the atoms. The small review presented in this paper shows that some significant progress has been achieved in the building of potentials thanks to *ab initio* calculations. In particular, we show that discrepancies between the properties predicted using different many-body potentials as well as by *ab initio* calculations have led to the generation of new potentials. These new potentials, based on *ab initio* data as input parameters in the fitting procedure, appear to be more suitable to simulate radiation damage or plasticity and examples for Fe and Zr are presented in this paper. These new potentials remain based on an EAM type formalism, which allows versatility to fit the data set used to build them. As the data obtained at the atomic level are often used in higher scale models (kinetic Monte Carlo, rate theory, dislocation dynamics) to obtain "macroscopic" properties, the improvement of the interatomic potentials thanks to *ab initio* calculations contributes to the improvement of multiscale modelling methods. To summarize, the development of adequate interatomic potentials is necessary for the materials science community and this paper underscores the fact that the use of *ab initio* calculations is necessary to obtain more accurate potentials.

Deleted: 5
Deleted: atomistic
Deleted:
Deleted:
Deleted:
Formatted
Deleted: D
Deleted: atomistic
Deleted: upper
Deleted: thus
Formatted

Acknowledgements

Part of this work was supported by the European project PERFECT (FI6O-CT-2003-508840).

Table captions

Table 1*: Comparison between USPP and PAW results for some energetic properties related to dilute Fe alloys. The mixing energies of Cu in Fe and of Ni in Fe were determined in 128-atom supercells with 27 k points, the binding energies between two Mn atoms in first and second nearest neighbour were calculated using a 54-atom supercell and 125 k points.*

List of Tables

	USPP	PAW
E_{mixing} (Cu → Fe) (eV)	0.55	0.82
E_{mixing} (Ni → Fe) (eV)	–0.12	0.24
E_{bind} (Mn – Mn 1nn) (eV)	–0.19	0.07
E_{bind} (Mn – Mn 2nn) (eV)	–0.21	0.03

Figure captions

Figure 1*: The two debated core structures of the 1/2a⟨111⟩ screw dislocation in α-Fe using Vitek's differential displacement method [**36**]. The length of an arrow is proportional to the displacement difference. The longest arrow corresponds to b/3. The different sphere colours indicate on which {111} plane the atoms lie.*

Figure 2: *DK formation along the dislocation line of a a/2⟨111⟩ screw dislocation in Fe submitted to a pure shear strain at 200 K [**39**]. The dislocation line is 160 $\vec{b}$ long. Pairs of atoms for which the relative displacement in the [111] direction is equal to or larger than b/3 are represented.*

Figure 3: *Interaction of a a/2⟨111⟩ screw dislocation interaction with(a) a nano-void containing 200 vacancies, (b) a ⟨111⟩ interstitial loop containing 61 SIAs at 300K. The last configuration of the dislocation before unpinning the irradiation defect is represented. The dislocation line is 160 $\vec{b}$ long. The dislocation line, the void and the loop are identified geometrically thanks to a local environment analysis of the first nearest neighbour atoms [**95**] (by adapting the fcc analysis to the bcc case). The coordination number of the represented atoms are; yellow:6, grey: 5, green 4 or lower.*

Formatted

Figure 4: *Typical aspect of a 20 keV cascade at 600K for three Fe potentials at the end of the recombination phase. Left hand side: the big empty circles are the replaced atoms, the big dark circles are the interstitials. Right hand side the dark circles are interstitials, the empty ones are vacancies. Box size 23 nm.*

List of figures

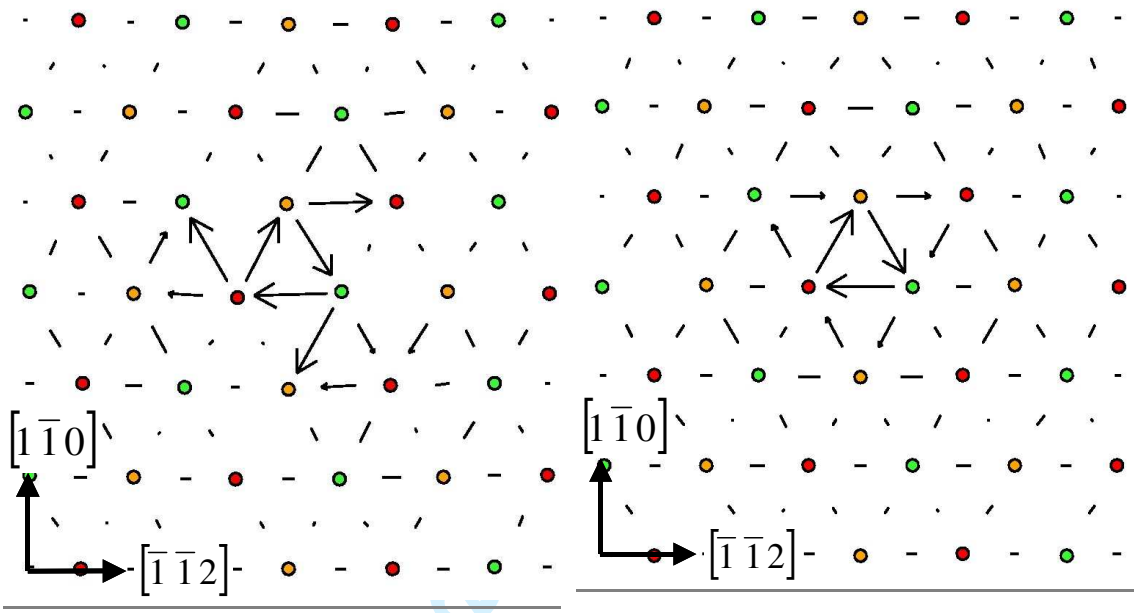

Extended core Compact core

Figure 1: *The two debated core structures of the 1/2a⟨111⟩ screw dislocation in α-Fe using Vitek's differential displacement method [36]. The length of an arrow is proportional to the displacement difference. The longest arrow corresponds to b/3. The different sphere colours indicate on which {111} plane the atoms lie.*

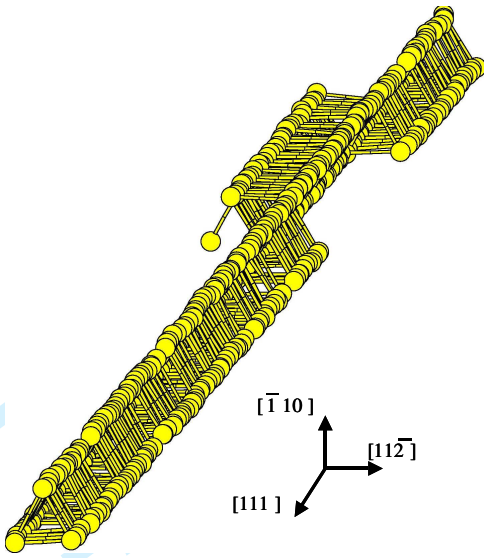

Figure 2: *DK formation along the dislocation line of a a/2⟨111⟩ screw dislocation in Fe submitted to a pure shear strain at 200 K [39]. The dislocation line is 160* $\vec{b}$ *long. Pairs of atoms for which the relative displacement in the [111] direction is equal to or larger than b/3 are represented.*

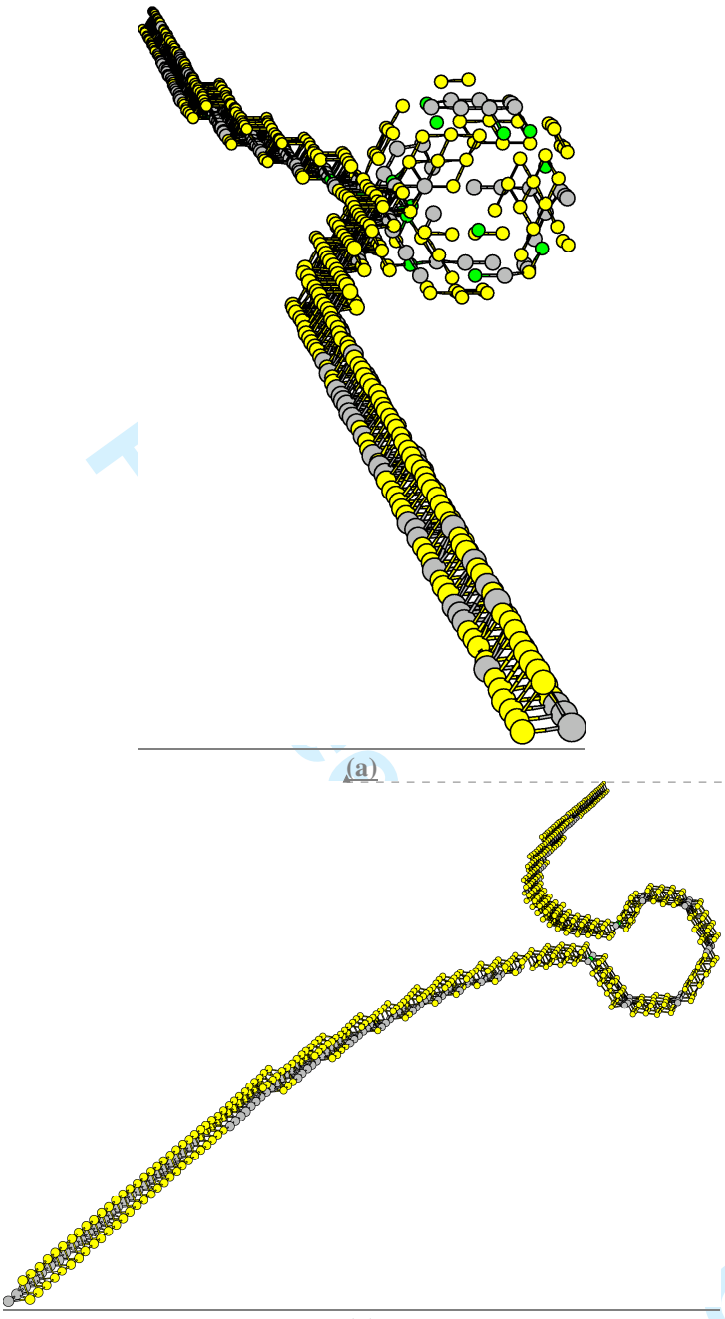

Figure 3: *Interaction of a a/2⟨111⟩ screw dislocation interaction with(a) a nano-void containing 200 vacancies, (b) a ⟨111⟩ interstitial loop containing 61 SIAs at 300K. The last configuration of the dislocation before unpinning the irradiation defect is represented. The dislocation line is 160* $\vec{b}$ *long. The dislocation line, the void and the loop are identified geometrically thanks to a local environment analysis of the first nearest neighbour atoms [95] (by adapting the fcc analysis to the bcc case). The coordination number of the represented*

Formatted

Formatted

Deleted: 95

Formatted

atoms are; yellow:6, grey: 5, green 4 or lower.

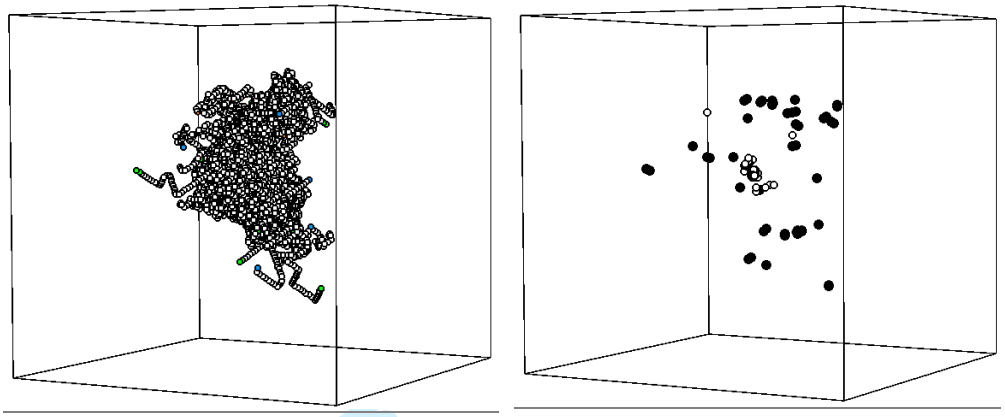

Fe I

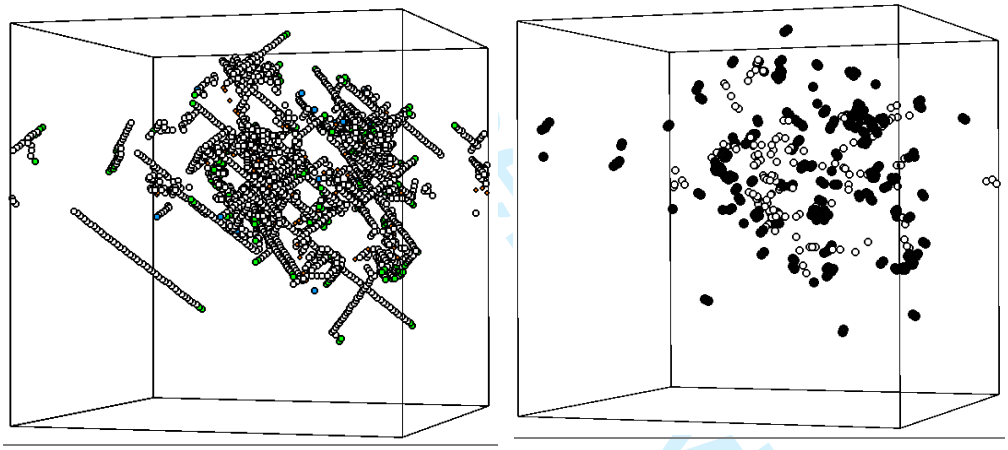

Fe II

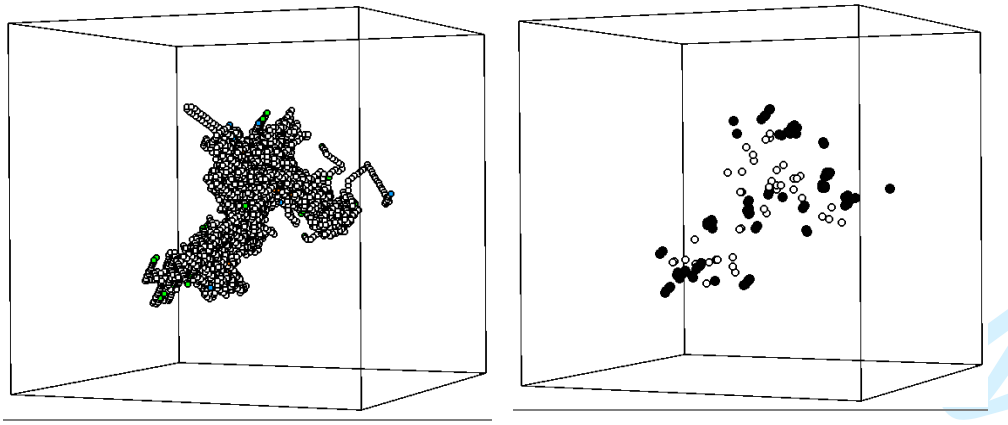

Fe III

Figure 4: *Typical aspect of a 20 keV cascade at 600K for three Fe potentials at the end of the recombination phase. Left hand side: the big empty circles are the replaced atoms, the big dark circles are the interstitials. Right hand side the dark circles are interstitials, the empty ones are vacancies. Box size 23 nm.*

References

[1] M.S. Daw and M.I. Baskes, Phys. Rev. Lett. **50** (1983) 1285.

[2] M.W. Finnis and J.E. Sinclair, Phil. Mag. A **50** (1984) 45.

[3] J.K. Norskov, Reports on Progress in Physics **53** (1990) 1253.

[4] F. Ducastelle and F. Cyrot-Lackmann, J. Phys. Chem. Solids **32** (1971) 285.

[5] V. Rosato, M. Guillopé and B. Legrand, Phil. Mag. A **59** (1989) 321.

[6] F. Ercolessi, E. Tosatti and M. Parinello, Surface Science **177** (1986) 314; Phys. Rev. Lett. **57** (1986) 719.

[7] J.B. Gibson, A.N. Goland, M. Milgram and G.H. Vineyard, Phys. Rev. **120** (1960) 1229.

[8] C. Erginsoy and G.H. Vineyard, A. Englert, Phys. Rev. **135** (1963) A595.

[9] A.F. Calder and D.J. Bacon, J. Nucl. Mater. **207** (1993) 25.

[10] W.J. Phythian, R.E. Stoller, A.J.E. Foreman, A.F. Calder and D.J. Bacon, J. Nucl. Mater. **223** (1995) 245.

[11] R.E. Stoller, G.R. Odette and B.D. Wirth, J. Nucl. Mater. **251** (1997) 49.

[12] F. Gao, D.J. Bacon, P.E.J. Flewitt and T.A. Lewis, J. Nucl. Mater. **249** (1997) 77.

[13] R.E. Stoller, J. Nucl. Mater. **276** (2000) 22.

[14] C.S. Becquart, C. Domain, A. Legris and J.C. van Duysen, J. Nucl. Mater **280** (2000) 73.

[15] E. Hornbogen and R.C. Glenn, Trans. Metall. Soc. Aime **218** (1960) 1064.

[16] C.S. Becquart, C. Domain and J.C. Van Duysen, J. Nucl. Mater. **294** (2001) 274.

[17] A.F. Calder and D.J. Bacon, MRS Proceedings, **439** (1997) 521.

[18] J.W. Jang, B.J. Lee and J.H. Hong, J. Nucl. Mater. **373** (2008) 28.

[19] A.F. Calder, D.J. Bacon, A.V. Barashev and Yuri N. Osetsky, J. Nucl. Mater. **382** (2008) 91.

[20] L. Yang, X. T Zu, H. Y. Xiao, F.Gao, K.Z. Liu, H.L. Heinisch, R.J. Kurtz and S.Z. Yang, Mater. Science & Eng., **A427** (2006) 343.

[21] L. Yang, X. T Zu, H. Y. Xiao, F.Gao, X. Y.Wang and K. Z. Liu, Mater. Science Forum **561-565** (2007) 1753.

[22] L. Yang, X. T Zu, H. Y. Xiao, F.Gao, H. L Heinisch and R.J. Kurtz, Physica B: Condensed Matter **391** (2007) 179.

[23] J. Yu, G. Yu, Z. Yao and R. Schaeublin, J. Nucl. Mater. **367-370** (2007) 462.

[24] G. Lucas and R. Schaublin, J. Phys.: Condensed Matter **20** (2008) 415206.

Deleted:

Deleted: ,

Deleted: 274

[25] J.Pu, L. Yang, F. Gao, H.L. Heinisch, R.J. Kurtz and X. T. Zu, Nucl. Instr. and Meth. in Phys. Res. **B. 266** (2008) 3993.

[26] H. Hurchand, S.D. Kenny, C.F. Sanz-Navarro, R. Smith and P.E.J. Flewitt, Nucl. Instr. and Meth. in Phys. Res. **B 229** (2005) 92.

[27] L. Malerba, D. Terentyev, P. Olsson, R. Chakarova and J. Wallenius, J. Nucl. Mater**. 329-333** (2004) 1156.

[28] D. Terentyev, L. Malerba, R. Chakarova, K. Nordlund, P. Olsson, M. Rieth and J. Wallenius, J. Nucl. Mater. **349** (2006) 119.

[29] J-H. Shim, H-J. Lee and B.D Wirth, J. Nucl. Mater. **351** (2006) 56.

[30] C. Björkas, K. Nordlund, L. Malerba, D. Terentyev and P. Olsson, J. Nucl. Mater. **372** (2008) 312.

[31] K. Vortler, C. Björkas, D. Terentyev, L. Malerba and K. Nordlund, J. Nucl. Mater. **382** (2008) 24.

[32] A.F. Calder, D.J. Bacon, A.V. Barashev and Y.N. Osetstky, Phil. Mag. Lett. **88** (2008) 43.

[33] C. Domain and C.S. Becquart, Phys. Rev. B **71** (2005) 214109.

[34] P. Olsson, C. Domain and J. Wallenius, Phys. Rev. B **75** (2007) 014110.

[35] R.E. Voskoboinikov, Y.N. Osetsky and D.J. Bacon, Mater. Sci. Eng. A, **400-401** (2005) 45.

[36] V. Vitek, Cryst. Latt. Def. **5** (1974) 1.

[37] Yu.N Osetsky. and D.J. Bacon, Modelling Simul. Mater. Sci. Eng. **11** (2003) 427.

[38] W. Cai, V. V. Bulatov and J. Marian, Nature Mater. **3** (2004)158.

[39] C. Domain and G. Monnet, Phys. Rev. Lett. **95** (2005) 215506.

[40] R.E. Voskoboinikov, Yu.N. Osetsky and D.J. Bacon, Mater. Sci. Eng. A, **400-401** (2005) 49.

[41] D. Terentyev, P. Grammatikopoulos, D.J. Bacon and Yu. N. Osetsky, Acta Mater. **56** (2008) 5034.

[42] C.S. Becquart, J.M. Raulot, G. Bencteux, C. Domain, M. Perez, S. Garruchet and H. Nguyen, Comp. Mater. Sci. **40** (2007) 119.

[43] C. Domain, C.S. Becquart and J. Foct, Phys. Rev. B **69** (2004) 144112.

[44] S. Garruchet and M. Perez, Comp. Mater. Sci. **43** (2008) 286.

[45] E. Clouet, S. Garruchet, H. Nguyen, M. Perez and C. S. Becquart, Acta mater. **56** (2008) 3450.

[46] L. P. Kubin, Reviews on the Deformation Behavior of Materials **1** (1976) 243.

[47] A. Seeger and P. Schiller, Acta Metall. **10** (1962) 348.

[48] M. I. Mendelev, S.W. Han, D. J. Srolovitz, G. J. Ackland, D.Y. Sun and M. Asta, Phil. Mag. **83** (2003) 3977.

[49] G.J. Ackland, M.I. Mendelev, D.J. Srolovitz, S. Han and A.V. Barashev, J. Phys: condens. Matter **16** (2004) 1.

[50] J. Marian, B. D. Wirth, R. Schaublin, G.R. Odette and J.M. Perlado, J. Nucl. Mater. **323** (2003) 181.

[51] D.J. Bacon and Y.N. Osetsky, Math. Mech. Sol. **14** (2009) 270.

[52] S. Jumel, J.-C. van Duysen, J. Ruste and C. Domain, J. Nucl. Mater. **346** (2005) 79.

[53] P.B. Hirsch, in: R.E. Smallman, J.E. Harris (Eds.), Proceeding of Vacancies 1976 (1977) 95.

[54]. D. Pramanik and D. N. Seidman, J. Appl. Phys. **54** (1983) 6352.

[55] D. N. Seidman, R. S. Averback, and R. Benedek, Phys. Stat. Solidi (b) **144** (1987) 85.

[56] J.F. Ziegler, J.P. Biersack, and U. Littmark, *Stopping Powers and Ranges of Ions in Matter* ~Pergamon, New York, 1985, p. 25.

[57] F. Maury, M. Biget, P. Vajda, A. Lucasson, and P. Lucasson, Phys. Rev. B **14** (1976) 5303.

[58] C.S. Becquart, C. Domain, A. Legris and J.C. van Duysen, *Multiscale Modelling of Materials*, edited by G.E. Lucas, L. Snead, M.A. Kirk, Jr., and R.G. Elliman, MRS Symposia Proceedings No. 650 ~Materials Research Society, Pittsburgh, 2001, p. R3.24.

[59] C.S Becquart, A. Souidi and M. Hou, Phys. Rev. **B, 66** (2002) 134104.

[60] D.A. Terentyev, C. Lagerstedt, P. Olsson, K. Nordlund, J. Wallenius, C.S. Becquart and L. Malerba, J. Nucl. Mater. **351** (2006) 65.

[61] C. Domain and C. S. Becquart, Phys. Rev. B **65** (2001) 024103/1-14.

[62] C. Bjorkas and K. Nordlund, Nucl. Inst. Meth. In Phys. Res. B **259** (2007) 835.

[63] S. Ismail-Beigi and T. A. Arias, Phys. Rev. Lett. **84** (2000) 1499.

[64] C. Woodward and S. I. Rao, Phys. Rev. Lett. **88** (2002) 216402.

[65] F. Gao, G. Henkelman, W.J. Weber, L.RL Corrales and H. Jónsson, Nucl. Instr. & Meth. B **202** (2003) 1.

[66] R.C. Pasianot, A.M. Monti, G. Simonelli and E.J. Savino, J. Nucl. Mater. **276** (2000) 230.

[67] Yu. N. Osetsky, Defect and Diffusion Forum, **188-190** (2001) 71.

Formatted

Formatted

[68] F. Gao, D. J. Bacon, A. V. Barashev and H. L. Heinisch, Mater. Res. Soc. Symp. Proc. **540** (1999) 703.

[69] B.D. Wirth, G.R. Odette, D. Maroudas and G.E. Lucas, J. Nucl. Mater. **244** (1997) 185.

[70] Yu. N. Osetsky, M. Victoria, A. Serra, S. I. Golubov, and V. Priego, J. Nucl. Mater. **251** (1997) 34.

[71] P. Ehrhart, K.H. Robrock and H.R. Schober, in: "Physics of Radiation Effects in Crystals", ed. R.A. Johnson and A.N. Orlov, Elsevier, Amsterdam (1986) 7, and references therein.

[72] S. Takaki, J. Fuss, H. Kugler, U. Dedek and H. Schultz, Rad. Eff. **79** (1983) 87.

[73] R.A. Johnson, Phys. Rev. **134** (1964) A1329.

[74] C.-C. Fu, F. Willaime and P. Ordejón, Phys. Rev. Lett. **92** (2004) 175503.

[75] L. Malerba, G.J. Ackland, C.S. Becquart, G. Bonny, C. Domain, S. Dudarev, C.-C. Fu, D. Hepburn, M.C. Marinica, P. Olsson, R.C. Pasianot, J.M. Raulot, F. Soisson, D. Terentyev, E. Vincent and F. Willaime, submitted to J. Nucl. Mater.

[76] D. A. Terentyev, L. Malerba and M. Hou, Phys. Rev. B **75** (2007) 104108.

[77] D.A. Terentyev, L. Malerba, P. Klaver and P. Olsson, Jour. Nucl. Mater. **382** (2008) 126.

[78] G. Lucas and L. Pizzagalli, Phys. Rev. B **72** (2005) 161202(R).

[79] E. Holmström, A. Kuronen, and K. Nordlund, Phys. Rev. B **78** (2008) 045202.

[80] T. Harry and D.J. Bacon, Acta Mater. **50** (2002) 195.

[81] C. Domain, R. Besson and A. Legris, Acta Mater. **52** (2004) 1495.

[82] F. Willaime and C. Massobrio, Phys. Rev. B **43** (1991) 11653.

[83] G.J. Ackland, S.J. Wooding and D.J. Bacon, Phil. Mag. A **71** (1995) 553.

[84] R.C. Pasianot and A.M. Monti, J. Nucl. Mater. **264** (1999) 198.

[85] A. Girshick, A.M. Bratkovsky, D. G. Pettifor and V. Vitek, Phil. Mag. A **77** (1998) 981.

[86] A. Girshick, D. G. Pettifor and V. Vitek, Phil. Mag. A, **77** (1998) 999.

[87] C. Domain and A. Legris, Proceedings of the IUTAM conference, Osaka 2003, Kluwer academic publishers, (2004) 411.

[88] B. Legrand, Phil. Mag. B **49** (1984) 171.

[89] M.I. Mendelev and G. J. Ackland, Phil. Mag. Lett. **87** (2007) 349.

[90] A. H. Khater, PhD University Liverpool (2008).

Formatted
Formatted
Formatted
Formatted
Formatted
Formatted
Formatted
Deleted: p

[91] M. Perez, F. Perrard, V. Massardier, X. Kleber, A. Deschamps, H. de Monestrol, P. Pareige and G. Covarel, Phil. Mag., **85**, (2005) 2197.

[92] P. Olsson, T.P.C. Klaver, C. Domain, submitted to Phys. Rev. B

[93] A. Vehanen, P. Hautojärvi, J. Johansson, J. Yli-Kauppila and P. Moser, Phys. Rev. B **25** (1982) 762.

[94] H.E Schaefer, K. Maier, M. Weller, D. Herlach, A. Seeger and J. Diehl, Scripta Met. **11** (1977) 803.

[95] D. Rodney, Acta mater. **52** (2004) 607.

Deleted: .
Formatted
Deleted: ,
Deleted: Vol.
Formatted
Deleted: No. 20
Formatted
Formatted
Formatted
Deleted: .
Deleted: Pär Olsson, private communication.
Deleted: ¶
Formatted
Formatted
Formatted